

BEHAVIOUR OF PLASMONIC NANOPARTICLE-GENERATED CAVITATION BUBBLES

EMIL-ALEXANDRU BRUJAN

Abstract. The transient dynamics of cavitation nanobubbles generated through the irradiation of gold nanoparticles, via the particle's plasmonic resonance, very close to the threshold laser fluence for bubble formation, is investigated numerically. Both for short and long laser pulses, the maximum bubble radius is in the nanometer range. The maximum bubble radius is almost proportional to the square root of the laser fluence. For long laser pulses, and very close to the threshold fluence for bubble formation, the energy dependence of the bubble size is stronger. The oscillation time of cavitation nanobubbles is smaller than that predicted by the Rayleigh formula. Excellent agreement was found between previous experimental results and the present calculations. The results indicate that the mechanical effects associated with bubble formation are compatible with intracellular nanosurgery and are also of interest for a gentle transfection of genes into biological cells.

Key words: bubble, nanoparticle, nonlinear dynamics, modeling and simulation.

1. INTRODUCTION

It was recently demonstrated that the mechanical properties of cavitation bubbles, generated through the irradiation of plasmonic gold nanoparticles, can be used to produce a surgical device. A cavitation bubble is induced when a plasmonic gold nanoparticle is overheated with a laser pulse. As a result, the nanoparticle evaporates a very thin volume of the surrounding medium, thus generating a cavitation bubble that grows and then collapses within a very short period of time. The fast expansion of the bubble generates a localized mechanical impact on the environment with only minor thermal contributions [1]. It was also showed that plasmonic nanoparticle-generated bubbles can be efficiently used at the cellular and tissue level *in vitro* and *in vivo* as therapeutic, delivery and theranostic agents [2, 3]. Cavitation bubbles can also aid diagnostics, for instance during imaging, as they may act as scattering centers for the probe.

“Politehnica” University Bucharest, Department of Hydraulics, Spl. Independentei 313, 060042 Bucharest, Romania

Rom. J. Techn. Sci. – Appl. Mechanics, Vol. 58, N° 3, P. 231–240, Bucharest, 2013

Although the thermalization of nanoparticles has been extensively studied [4], the dynamics of plasmonic nanoparticle-generated bubbles are less explored. Several theoretical studies have been conducted to investigate the initial phase of bubble formation around laser-irradiated nanoparticles and microparticles [5,6]. A recent publication [7] describes the formation of a cavitation bubble around a plasmonic nanoparticle in which an expression for the acoustic wave pressure as a function of laser pulse energy is given.

In any applications of plasmonic nanoparticles it is important to understand and control the spatial and temporal behaviour of cavitation bubbles in the liquid around nanoparticles. In a previous study [8] we have described the dynamics of cavitation bubbles at values of the laser fluence much larger than the threshold value for bubble formation. The present study describes numerical investigations of the dynamics of cavitation bubbles generated around gold nanoparticles irradiated with laser pulses at fluence values very close to the threshold value for bubble formation. We used a spherical model of bubble dynamics valid to first-order in the bubble wall Mach number. The effects of nanoparticle radius, laser fluence, and pulse duration on the maximum radius and oscillation time of the nanobubbles are discussed. Model predictions are then compared with the available experimental results.

2. MATHEMATICAL FORMULATION

Consider a spherical gold nanoparticle of radius R_{np} suspended in a liquid of infinite extent and irradiated by a laser pulse with duration τ_L . When a certain laser fluence threshold is reached, the temperature of the nanoparticle exceeds the boiling point of the host liquid, and a vapour layer is formed on the surface of the nanoparticle. The large pressure in the vapour layer surrounding the bubble leads to a very rapid expansion of the layer with subsequent formation of a cavitation bubble. A spherical model of bubble dynamics is used to calculate the temporal development of the bubble radius [9]. The model considers the compressibility of the liquid, surface tension and the liquid viscosity. The bubble dynamics is described by the equation

$$R\ddot{R} + \frac{3}{2}\dot{R}^2 - \frac{1}{c_\infty}\left(R^2\ddot{R} + 6R\dot{R}\ddot{R} + 2\dot{R}^3\right) = H, \quad (1)$$

where R is the time-dependent bubble radius, dots denote a time derivative, c_∞ is the undisturbed speed of sound in the medium and H is the enthalpy change between bubble wall and infinity,

$$H = \frac{n(p_0 + B)}{(n-1)\rho_0} \left[\left(\frac{P + B}{p_0 + B} \right)^{(n-1)/n} - 1 \right]. \quad (2)$$

The constants B and n relate to the Tait equation of state for water that was used to derive Eq. (2). The pressure P at the bubble interface is

$$P = \left(p_0 + \frac{2\sigma}{R_0} \right) \left(\frac{R_0^3 - R_{np}^3}{R^3 - R_{np}^3} \right)^\kappa - \frac{2\sigma}{R} - 4\eta \frac{\dot{R}}{R}. \quad (3)$$

Here R_0 denotes the initial radius of the bubble, κ the ratio of the specific heat at constant pressure and volume, p_0 the initial pressure inside the bubble, σ the surface tension and η the medium viscosity.

Assuming that the excess light energy absorbed by the particle during the laser pulse is spent in boiling at the critical point of water, the initial radius of the bubble can be estimated as [7]

$$R_0 = \left\{ \frac{3}{4\pi\rho_{cl}} \left[\frac{(F - F_c)\sigma_{abs}}{E_{cl}} \right] + R_{np}^3 \right\}^{1/3}. \quad (4)$$

In the above equation, E_{cl} is the internal energy of the liquid at the critical point, ρ_{cl} is the critical density of the liquid, σ_{abs} represents the absorption cross section, F is the laser fluence, and F_c is the critical laser fluence required to heat the nanoparticle to the boiling temperature T_{boil} , which in the case of short laser pulses ($\chi_l\tau_L \ll R_{np}^2$, where χ_l is the thermal diffusivity of the liquid) is given by [7]

$$F_c = V_{np}c_{np}\rho_{np}T_{boil} / \sigma_{abs}. \quad (5)$$

For long laser pulses ($\chi_l\tau_L \gg R_{np}^2$), the expression for the critical laser fluence becomes [7]

$$F_c = 4\pi R_{np}c_l\rho_l\chi_l\tau_L T_{boil} / \sigma_{abs}. \quad (6)$$

In the numerical calculations we take $B = 3049.13$ bar and $n = 7.15$ in the equation of state of the liquid. Other pertinent numerical values are $\kappa = 1.4$, $E_{cl} = 2000$ kJ/kg, $p_0 = 101325$ Pa, $\rho_l = 998$ kg/m³, $\rho_{cl} = 322$ kg/m³, and $\sigma = 0.07$ N/m, $c_{np} = 0.13$ kJ/(kg·K), $c_l = 4.18$ kJ/(kg·K), $\rho_{np} = 19300$ kg/m³, and $\chi_l = 1.4 \cdot 10^{-7}$ m²/s. The temperature and the pressure inside the initial bubble are those at the critical point of water ($T_{cl} = 647.1$ K, $p_{cl} = 22.06$ MPa).

3. RESULTS AND DISCUSSION

Figure 1 illustrates the temporal variation of the radius of cavitation bubbles generated from a spherical gold nanoparticle with a radius of 20 nm. The most prominent feature of the transient cavitation bubbles is their small size and short

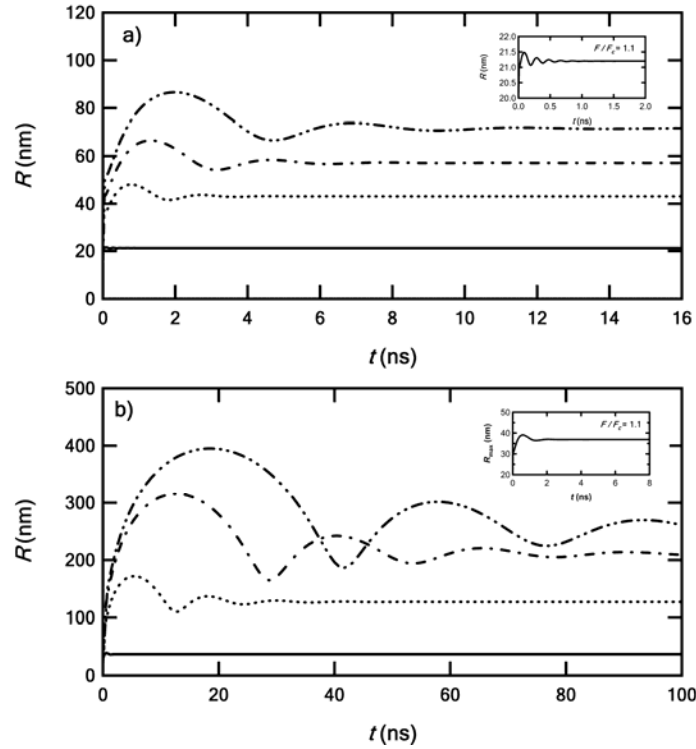


Fig. 1 – Variation with time of the radius of cavitation bubbles generated after laser irradiation of a spherical gold nanoparticle with radius $R_{np} = 20$ nm, for various values of the ratio F/F_c : a) bubbles generated from short laser pulses; b) bubbles generated from a long laser pulse with duration $\tau_L = 10$ ns. Solid line: $F/F_c = 1$; dotted line: $F/F_c = 4$; dashed line with one point: $F/F_c = 7$; dashed line with two points: $F/F_c = 10$. The inset shows the bubble radius as a function of time for $F/F_c = 1.1$.

lifetime. For example, the maximum radius, R_{max} , of the bubble generated from a nanoparticle irradiated with a laser pulse of 10 ns at $F/F_c = 10$ amounts to only 395 nm in water, and will be even smaller in a viscoelastic medium such as the cytoplasm. Such small bubbles are similar to those generated by focusing femtosecond laser pulses in the bulk of a liquid [10]. They are, however, three order of magnitude smaller than the bubbles generated by nanosecond optical breakdown in water ($R_{max} > 0.5$ mm for $\tau_L = 6$ ns) [11]. For the smallest value of the laser fluence used in the present calculations ($F/F_c = 1.1$) the oscillation becomes strongly damped. For example, in the case of long laser pulses, the maximum bubble radius is 38.4 nm and only two oscillation cycles can be seen. For short laser pulses, the maximum bubble radius is smaller with a factor of 5 for $F/F_c = 10$ ($R_{max} = 85$ nm), and with a factor of 2 for $F/F_c = 1.1$ ($R_{max} = 21.5$ nm). This makes a dissection mechanism associated with bubble formation compatible with intracellular nanosurgery because such small bubbles are essential to dissect

or knock out subcellular structures with nanometer precision. They are also of great interest for a gentle transfection of genes and transfer of other substances into specific cell types [12]. On the other hand, the small size of these bubbles is consistent with the fact that the collective action of a large number of nanoparticles is required to produce cell lysis.

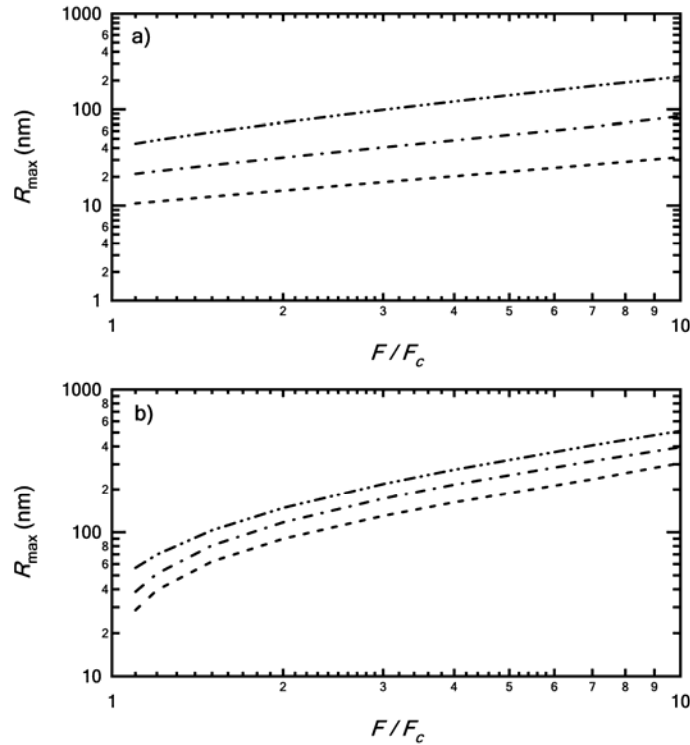


Fig. 2 – Maximum bubble radius as a function of the ratio, F/F_c , for various values of the nanoparticle radius, R_{np} : a) bubbles generated from short laser pulses; b) bubbles generated from a long laser pulse with duration $\tau_L = 10$ ns. Dashed line: $R_{np} = 10$ nm; dashed line with one point: $R_{np} = 20$ nm; dashed line with two points: $R_{np} = 40$ nm.

Figure 2 presents the maximal bubble radius as a function of the ratio F/F_c . At equal laser fluence, the maximum radius of the cavitation bubble decreases with decreasing nanoparticle radius and pulse duration. For example, for short laser pulses and $F/F_c = 4$, the maximum radius of the bubble generated from a nanoparticle with $R_{np} = 10$ nm ($R_{max} = 20.3$ nm) is with a factor of 6 smaller than for $R_{np} = 40$ nm ($R_{max} = 121.2$ nm). The corresponding values for a long laser pulse ($\tau_L = 10$ ns) are $R_{max} = 162$ nm, for $R_{np} = 10$ nm, and $R_{max} = 274.5$ nm, for $R_{np} = 40$ nm, respectively. For $F/F_c > 2$, the $R_{max}(F/F_c)$ dependence is generally not very strong, and even for the largest nanoparticle ($R_{np} = 40$ nm) irradiated at the

largest laser fluence ($F = 10F_c$), R_{\max} is much smaller than the size of a biological cell. For example, the largest value of the maximal bubble radius is 514 nm and was obtained for $R_{np} = 40$ nm and long laser pulses. Bubbles will be even smaller in cells where they are confined by the cytoskeleton [13]. The scaling law for the bubble size is the same for both short and long laser pulses and all values of R_{np} , namely, the maximum bubble radius is proportional to the square root of the laser fluence. This is in contrast to the case of large bubbles ($R_{\max} > 1$ mm), generated by nanosecond optical breakdown in water, where the maximum bubble radius is proportional to the cube root of the laser pulse energy [11]. For long laser pulses ($\tau_L = 10$ ns), this scaling law applies, however, only for $F/F_c > 2$. Closer to the threshold, the energy dependence of the bubble size is stronger. A similar trend was experimentally observed by Siems et al. [14] for 60 nm gold nanoparticles irradiated with nanosecond laser pulses.

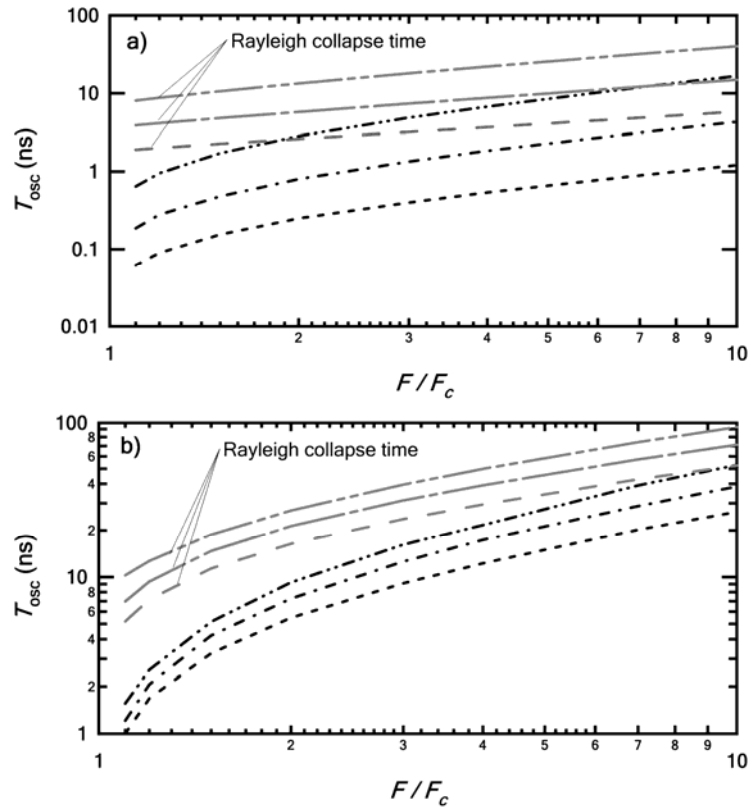


Fig. 3 – Oscillation time of a bubble as a function of F/F_c , for various values of R_{np} :
a) bubbles generated from short laser pulses; b) bubbles generated from a long laser pulse with duration $\tau_L = 10$ ns. Dashed line: $R_{np} = 10$ nm; dashed line with one point: $R_{np} = 20$ nm; dashed line with two points: $R_{np} = 40$ nm.

It is also interesting to note that the oscillation time of cavitation nanobubbles is smaller than that predicted by the Rayleigh formula [15]

$$T_{osc}^R = 1.83 \left(\frac{\rho_l}{\rho_0} \right)^{1/2} R_{max} . \quad (7)$$

Figure 3 illustrates the collapse time of the nanobubbles in comparison to the Rayleigh collapse time, both for the case of short (Fig. 3a) and long (Fig. 3b) laser pulses. For a nanoparticle radius $R_{np} = 20$ nm irradiated with a laser pulse with duration $\tau_L = 10$ ns at a fluence $F/F_c = 4$, the oscillation time of the resulting nanobubble is 12.6 ns, which is less than half the value predicted by the Rayleigh formula (31.3 ns). The corresponding value obtained in the case of short laser pulses is 1.34 ns, with a factor of 6 smaller than the value predicted by the Rayleigh formula (7.4 ns). The differences become larger with decreasing laser fluence and nanoparticle size. For large bubbles, as those generated by nanosecond or picosecond laser pulses in the bulk of a liquid, the expansion and collapse of cavitation bubbles are highly symmetrical and R_{max} can be calculated from T_{osc} using Eq. (7) [11]. However, for bubbles with maximum radii smaller than a few micrometers the Rayleigh equation is not exact because it neglects surface tension and the viscosity of the medium surrounding the bubble. Both factors produce a pressure scaling with $1/R$ which adds to the hydrostatic pressure. This finding leads to the conclusion that, in the case of nanobubbles, the use of the Rayleigh oscillation time to determine the bubble size, as done in previous studies [16], leads to an underestimation of the maximum bubble size.

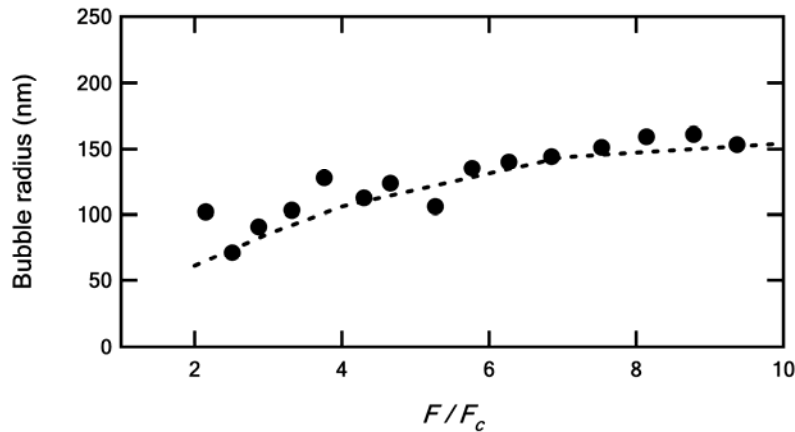


Fig. 4 – Comparison between simulated (dashed line) and experimental (filled symbols) results for the case of spherical gold nanoparticles with radius of 39 nm, irradiated with a short laser pulse $\tau_L = 100$ fs, in water, at a delay of maximum bubble radius of 650 ps.

A comparison between simulated and experimental results obtained by Kotaidis et al. [17], for the case of spherical gold nanoparticles with radius of 39 nm, irradiated with a short laser pulse ($\tau_L = 100$ fs), in water, is shown in Fig. 4. Very good agreement was found between experimental and numerical results. This implies, of course, that the neglected factors have little influence on the bubble dynamics or at least that some of the effects neutralize each other. It is interesting to note here that this model assumes that all the excess energy beyond heating the nanoparticle to the critical point is spent on boiling and used for forming the initial bubble. In the case of nanoparticles irradiated not under thermal confinement conditions, a large volume around the particle might be heated. Since the thermal gradient is very smooth, a significant heated volume might not reach the critical point. This heat cannot be used for forming the initial bubble and is lost. We also note that far above the threshold irradiation, F_c , the bubble can also nucleate during the laser pulse, which might lead to thermal insulation between the particle and the fluid by the vapour inside the bubble during the laser pulse as well as to optical scattering of the incident light. In this case, again, not all the applied laser pulse energy can be used to vaporize the liquid surrounding the nanoparticle. Therefore, the present model can only be used as an upper estimation limit for the bubble size. On the other hand, the surface tension of water is decreasing strongly with temperature until it vanishes at the critical point (see, for example, IAPWS Release on Surface Tension of Ordinary Water Substance, available at www.iapws.org), which can lead to larger bubbles than assumed in the model. Despite the desirable theoretical refinements that would be necessary to provide a complete description of bubble motion, the present formulation still gives a reasonable quantitative picture of bubble dynamics, and thus provides an essential practical connection between theory and experiment.

Recent years have seen a continuous rise of interest in nanosurgery on a cellular and sub-cellular level. One important application is the separation of individual cells or other small amounts of biomaterial from heterogeneous tissue samples for subsequent genomic or proteomic analysis. According to the present results, when suitable laser parameters are used, the resulting cavitation bubble is in the nanometer range, and surgery can be performed at any desired location within a cell or a very small organism. It is worth noting here that time-resolved investigations of the behaviour of laser-induced nanobubbles around gold nanoparticles within cells are not yet available. However, Dayton et al. [19] investigated the oscillations of bubbles with a radius of 1.5 μm that were phagocytosed by leukocytes. By means of streak photography and high-speed photography with 100 million frames/s they observed that phagocytosed bubbles expanded about 20 – 40% less than free. The difference is due to the viscoelastic properties of the cytoplasm and cytoskeleton. This however remains a potentially important point that will form the object of a separate investigation.

4. CONCLUSION

The dynamics of cavitation nanobubbles, generated after irradiation of spherical gold nanoparticles with laser pulses close to the threshold value for bubble formation, was investigated by numerical calculations. The significant parameters of this study are the nanoparticle radius, R_{np} , the laser fluence normalized by the threshold value for bubble formation, F/F_c , and the laser pulse duration. The maximum bubble radius increases with increasing nanoparticle radius, pulse duration and laser fluence. For $F/F_c < 10$, both for short and long laser pulses, the maximum bubble radius is in the nanometer range. For the smallest value of the laser fluence used in the present calculations ($F/F_c = 1.1$) the oscillation becomes strongly damped. This makes a dissection mechanism associated with bubble formation compatible with intracellular nanosurgery and is also of great interest for a gentle transfection of genes and into specific cell types. For laser fluences larger than the threshold value for bubble formation, the maximum bubble radius scales with the square root of laser fluence. This is in contrast to the case of large bubbles ($R_{max} > 1$ mm) generated by nanosecond optical breakdown in water where the maximum bubble radius is proportional to the cube root of the laser pulse energy. For long laser pulses and closer to the threshold, the energy dependence of the bubble size is stronger. The oscillation time of cavitation nanobubbles is smaller than that predicted by the Rayleigh formula. Thus, in the case of nanobubbles, the use of the Rayleigh oscillation time leads to an underestimation of the maximum bubble size. The Rayleigh equation cannot describe the oscillation time of bubbles smaller than a few micrometers because it neglects surface tension and viscosity that produce a pressure scaling with $1/R$ which adds to the hydrostatic pressure. The experimental data agree very well with the present numerical results.

Acknowledgements. This work was supported by a grant of the Romanian National Authority for Scientific Research, CNCS – UEFISCDI, project number PN-II-ID-PCE-2011-3-0079.

Received on September 29, 2013

REFERENCES

1. LAPOTKO, D., *Pulsed photothermal heating of the media during bubble generation around gold nanoparticles*, J. Heat Mass Transf., **52**, pp. 1540–1543, 2009.
2. KHLEBTSOV, B.N., ZHAROV, V.P., MELNIKOV, A.G., TUCHIN, V.V., KHLEBTSOV, N.G., *Optical amplification of photothermal therapy with gold nanoparticles and nanoclusters*, Nanotechnology, **17**, pp. 5167–5179, 2006.
3. LUKIANOVA -HLEB, E.Y., SAMANIEGO, A.P., WEN, J., METELITSA, L.S., CHANG, C.C., LAPOTKO, D.O., *Selective gene transfection of individual cells in vitro with plasmonic nanobubbles*, J. Control. Release, **152**, pp. 286–293, 2011.
4. HARTLAND, G.V., *Measurements of the material properties of metal nanoparticles by time-resolved spectroscopy*, Phys. Chem. Chem. Phys., **6**, pp. 5263–5274, 2004.
5. SCHMID, T., *Photoacoustic spectroscopy for process analysis*, Anal. Bioanal. Chem., **384**, pp. 1071–1086, 2006.
6. VOLKOV, A.N., SEVILLA, C., ZHIGILEV, L.V., *Numerical modelling of short pulse laser interaction with Au nanoparticle surrounded by water*, Appl. Surf. Sci., **253**, pp. 6394–6399, 2007.

7. EGEREV, S., ERMILOV, S., OVCHINNIKOV, O., FOKIN, A., GUZATOV, D., KLIMOV, V., KANAVIN, A., ORAEVSKY, A., *Acoustic signals generated by laser-irradiated metal nanoparticles*, *Appl. Opt.*, **48**, C38–C45, 2009.
8. BRUJAN, E.A., *Numerical investigation on the dynamics of cavitation nanobubbles*, *Microfluid. Nanofluid.*, **11**, pp. 511–517, 2011.
9. BRUJAN, E.A., *Collapse of cavitation bubbles in blood*, *Europhys. Lett.*, **50**, pp. 175–181, 2000.
10. VOGEL, A., NOACK, J., HUTTMAN, G., PALTAUF, G., *Mechanisms of femtosecond laser nanosurgery of cells and tissues*, *Appl. Phys. B*, **81**, pp. 1015–1047, 2005.
11. BRUJAN, E.A., *Dynamics of shock waves and cavitation bubbles in bilinear elastic-plastic media and the implications to short-pulsed laser surgery*, *Eur. Phys. J. Appl. Phys.*, **29**, pp. 115–123, 2005.
12. ANDERSON, L.J.E., HANSEN, E., LUKIANOVA-HLEB, E.Y., HAFNER, J.H., LAPOTKO, D.O., *Optically guided controlled release from liposomes with tunable plasmonic nanobubbles*, *J. Control. Release*, **144**, pp. 151–158, 2010.
13. HUTSON, M.S., MA, X., *Plasma and cavitation dynamics during pulsed laser microsurgery in vivo*. *Phys. Rev. Lett.*, **99**, 158104, 2007.
14. SIEMS, A., WEBER, S.A.L., BONEBERG, J., PLECH, A., *Thermodynamics of nanosecond nanobubble formation at laser-excited metal nanoparticles*, *New J. Phys.*, **13**, 043018, 2011.
15. RAYLEIGH, Lord, *On the pressure developed in a liquid during the collapse of a spherical cavity*, *Phil. Mag.*, **34**, pp. 94–98, 1917.
16. WAGNER, D.S., DELK, N.A., LUKIANOVA-HLEB, E.Y., HAFNER, J.H., FARACH-CARSON, M.C., LAPOTKO, D.A., *The in vivo performance of plasmonic nanobubbles as cell theranostic agents in zebrafish hosting prostate cancer xenografts*, *Biomater.*, **31**, pp. 7567–7574, 2010.
17. KOTAIDIS, V., DAHMEN, G., VON PLESSEN, G., SPRINGER, F., PLECH, A., *Excitation of nanoscale vapor bubbles at the surface of gold nanoparticles in water*, *J. Chem. Phys.*, **124**, 184702, 2006.
18. DAYTON, P.A., CHOMAS, J.E., LUNN, A.F.H., ALLEN, J.S., LINDNER, J.R., SIMON, S.L., FERRARA, K.W., *Optical and acoustical dynamics of microbubble contrast agents inside neutrophils*, *Biophys. J.*, **80**, pp. 1547–1556, 2000.